NPL REPORT CIRM 50

Energy resolution of in-phantom dose and charge measurement techniques used in the reconstruction of electron spectra

R. P. Hugtenburg, A. R. DuSautoy and S. Duane

Centre for Ionising Radiation Metrology

February 2002

NPL REPORT CIRM 50

February 2002

Energy resolution of in-phantom dose and charge measurement techniques used in the reconstruction of electron spectra

R. P. Hugtenburg[1] A. R. DuSautoy[2] and S. Duane[2]

1. Department of Medical Physics and Clinical Engineering
University Hospital Birmingham NHS Trust
Birmingham, West Midlands
B15 2TH
United Kingdom

2. Centre for Ionising Radiation Metrology
National Physical Laboratory
Teddington, Middx
TW11 0LW
United Kingdom

ABSTRACT

The energy resolution of spectra derived from dose and charge versus depth measurements performed in a uniform water phantom are examined. A Markov chain Monte Carlo (MCMC) method has been devised to determine spectra for broad parallel electron beams. The MCMC method presented here is an example of an inverse Monte Carlo method. MCMC is able to consider the contribution of electrons sampled from a prior continuous energy domain. Minimum resolutions acquired for pre-computed dose and charge distributions of 10 MeV electrons are 0.28 MeV and 0.59MeV respectively. The resolution of pre-computed bi-energetic sources are demonstrated and realistic beam spectra are examined for two therapeutic linear accelerators.

ISSN 1369-6793

National Physical Laboratory
Teddington, Middlesex, United Kingdom, TW11 0LW

Approved on behalf of the Managing Director, NPL
by Martyn Sené, Head of Centre for Ionising Radiation Metrology

Introduction

This is a short study examining resolution limits to the reconstruction of electron spectra from in-phantom dose and charge distributions. Another means of determining electron spectra is magnetic spectrometry [1, 2, 3, 4] but this equipment is not likely to be available to radiation workers, particularly in a radiotherapy setting. Calculations will be presented that are based on the inverse Monte Carlo method [5, 6]. Here the usual forward Monte Carlo method is extended so that dose and charge distributions, computed for an absorbing medium, are compared with measurements and weighted accordingly. The technique is similar to importance sampling in this respect. A comparable technique, the determination of megavoltage photon spectra from transmission measurements, is reasonably accurate [7, 8, 9, 10, 11, 12] though, as scatter in the absorbing materials can be minimised, Monte Carlo or comparable methods are not required. Only a few workers [13, 14, 15, 16, 17, 18] have demonstrated such methods for the reconstruction of electron spectra.

Two types of the inverse Monte Carlo method will be described here, iterative and non-iterative. The non-iterative inverse method requires that the phase space domain and the spatial distribution of dose or charge be parameterised to form a kernel. The iterative inverse method, also known as Markov chain Monte Carlo (MCMC) enables particles to be sampled from a continuous phase-space domain. The method has been used here to examine potential energy resolution limits as it is preferable not to discretise the spectral domain. A large sample space in the phase-space of a beam, such as would be encountered with scattering or degrading applicators in electron radiotherapy, may be another motivation to avoid discretisation.

For the general problem of spectrum unfolding, the non-iterative inverse method is very useful and for this reason it is described below.

Methods

Non-iterative inverse Monte Carlo

The non-iterative inverse method determines a matrix kernel, T, defined by

$$T\mathbf{w} = \mathbf{m} \tag{1}$$

where $\mathbf{w}$ is a set of weightings and $\mathbf{m}$ the measured data. T is therefore made up of columns consisting of dose or charge distributions computed for each element in a discrete set of incident particles. The system described in equation 1 is solved bearing in mind the positivity constraint on the weightings, $\mathbf{w}$, and distribution, $\mathbf{m}$. In general the problem is ill-conditioned, so a

set of spectral weightings $\{\mathbf{w}\}$ will satisfy the equation within some degree of tolerence. The choice of grid size will be influenced by the quality (spatial resolution) of the measured data.

As such the electron range is finite and, to a reasonable approximation, range related parameters such as R_p and R_{50} [19] are a linear function of beam energy. Consequently the matrix, T, approximates an upper-triangular or Row-Echelon form and comes into a class of problems that are easily solved using a back-substitution or stripping technique. The implication is that broad electron beams should characterise well the electron spectra that contribute to them.

Two approaches are recommended to solve equation 1. Firstly, simulated annealing and/or simplex methods [20] are useful in that a minimising least-squares function can be sought that includes a positivity constraint. Secondly, maximum likelihood methods [21, 22, 23, 24, 25] demonstrate good convergence properties and are easy to implement.

Iterative inverse/ Markov chain Monte Carlo

The Markov chain Monte Carlo (MCMC) method [26, 27] can be used to find a stable minimum difference between an expected or measured result and a series of estimates. This is the basis of the simulated annealing algorithm [28]. If the estimate is constructed from a conditional series of Monte Carlo results generated from a prior distribution, the technique is called the iterative inverse or reverse Monte Carlo method [29].

In our implementation, a prior phase space distribution is sampled and Monte Carlo dose and charge distributions are generated. Discrepencies between the simulated and measured distributions, in terms of a sum of square differences, are compared to the variance. Unlikely departures are rejected on a basis of their statistical significance. Because only a finite number of histories, h, are sampled per iteration, the rejection may be unfounded. This effect introduces a bias to the Monte Carlo method and will lead to an error in the computation if uncorrected. An increased number of runs of the same particle will ultimately confirm its place in a distribution.

The advantage of the iterative method is that it is not necessary to store a kernel, nor is it necessary to discretise the problem. It is particularly well suited to problems that are required to be solved only once. In radiotherapy treatment set-ups, anatomies can differ greatly from patient to patient, hence the potential for the use of such methods in this context.

In this paper we are interested in the resolution of energy spectra determined from dose and charge versus depth distribution and to begin with we will examine a monoenergetic (10 MeV) source. The peak is broadened by

process inherent to the measurement technique and by the method of inversion. The output from the iterative technique is a series of incident particles most likely to contribute to the monoenergetic distribution. The resolution can been assessed by computing a mean energy and standard deviation for this series. For a normal distribution the full-width-half-maximum (FWHM) of the peak is proportional to the standard deviation.

Implementation

Dose and charge distributions are computed using EGS4 [30] with the FIXTMS option [31] (ESTEPE = 0.01, PCUT = 0.100 MeV, ECUT = 0.611 MeV). The simulated geometry is a water phantom of 20 cm diameter and 30 cm depth. An electron is incident as a pencil beam with an energy sampled from an appropriate range. Dose and charge are scored within 200 20 cm diameter slabs, typically 0.5 mm thick. The acquired data is thus equivalent to a dose or charge versus depth distribution for broad-parallel beam.

Dose is calculated in terms of energy deposited (by accumulating EDEP in the subroutine AUSGAB). Charge is handled in the HOWFAR routine in the following manner. If at the end of the HOWFAR subroutine it is determined that a boundary is to be crossed then the charge of the current particle is subtracted from the old region and added to the new region. The charge of each incident electron must be added to the initial region prior to calling SHOWER.

Variance is also computed and is essential to the operation this MCMC method. It is the variance that provides the iterative scheme with a "cooling" schedule that gradually admits better estimates to the solution. The variance improves as $1/n$, where n is the iteration number, so the method has similarities to the fast-simulated annealing method [32, 33].

Variance is determined, on-the-fly, by accumulating the square of the deposited dose or charge at the end of each iteration. In this manner the probability of an event occuring in any particular slab, where the incident particle is sampled from a random distribution, is constant and the energy or charge deposited in each phantom slab is therefore Poisson distributed.

At the nth iteration the algorithm is described as follows:

1. A sample is taken from the set defining by our prior knowledge of the incident beam. Here an electron of incident energy, ε^n, is sampled from a range of possible values.

2. The particle transport is calculated h times and the energy or charge deposition, T_ε added to a discrete array, $S^n(z_l) = S^{n-1}(z_l) + T_\varepsilon(z_l)$.

l is a scoring region (at a particular depth z_l) in the scoring array. $l = 1, 2, ..., l_{\max}$ where $l_{\max}$ is the size of the array.

3. Concurrently an array of variances, $(\sigma^2)^n(z_l)$, is updated.

4. A Δ^2 value is determined from the sum over the scoring array for squares of differences between the accumulated result $S^n(z_l)$ and a set of measurements, $M(z_l)$.

$$\Delta^2 = \sum_l |S^n(z_l) - M(z_l)|^2 \tag{2}$$

   The calculation and measurement are normalised so that the integral of the energy or charge deposited over all z is 1. The normalisation at each step can be determined most efficiently by subtracting the quantity of dose or charge that leaves the dose scoring region from the incident kinetic energy of the particle (energy conservation must therefore be assured).

5. Likewise a total variance, $\sigma^2 = \sum_l (\sigma^2)^n(z_l)$ is determined

6. If Δ^2 is less than σ^2, the candidate is accepted, the values of n, ε, Δ^2 and σ^2 are output and n is incremented.

As the algorithm proceeds, the variance reduces and the acceptance criterion becomes more stringent until only particles that are sufficiently near to the distribution are being accepted. Note that from a performance point of view, the summations over the scoring arrays are costly and a Δ^2 and σ^2 updated at each energy deposition (in, say, AUSGAB) would be preferable.

The finite size of h introduces a bias into the calculation which means that outliers have some probability of contributing to the spectrum in accordance with the statistical test used to compute its probability of belonging to the distribution. This leads to a broadening of the spectrum beyond that which can be ascribed to the inherent resolution of the problem. Improving the variance for the comparative steps by increasing the number of histories per iteration is more successful than tightening the acceptance criterion.

In practice it is difficult to accurately determine the variance for the first few iterations and the algorithm can stall under these circumstances particularly if the spectrum is broad or has special features. The number of histories per iteration, h, may need to be increased slowly until it reaches a satisfactory value and equilibrium conditions are met. The collection of output from the algorithm is delayed until satisfactory levels of variance are reached (say, in comparison with the experimental uncertainty) and h is

at a level appropriate to the resolution of the problem. The length of the initialisation is called the "burn-in" period, n_b [34].

It is the issue of having to predetermine special parameters in Markov chain and simulated annealing methods that often generates criticism. The above formulation has no special "cooling schedule" as the reduction in the size of the stochastic step is enforced by the natural mode of summation of the Monte Carlo method. Instead only two parameters, h and n_b must be optimised for the problem at hand.

The efficiency of the method depends on the hit-rate, which is the proportion of histories admitted into the solution. If a highly peaked distribution is to be determined from a broad sampling range then the efficiency will be poor. The hit-rate decreases as h is increased and stabilises as the system approaches equilibrium, providing a means to assess appropriate values of h and n_b.

It turns out that the variance per history for a charge distribution is greater than for dose. The deposition of charge by electrons is comparable to the deposition of energy by photons in that it is localised. Realistic electron beams have been studied where it is difficult to separate the electron and photon components. In this case we introduce electron and photon histories with equal weightings of accumulated dose but substantially different variances. The algorithm appears to handle this circumstance.

In the following section, results for the MCMC method will be presented that have differing burn-in periods and differing histories per step. Here we are attempting to determine a resolution for spectra derived from dose or charge versus depth distributions for a broad beam which we represent in terms of a FWHM.

Results

Monoenergetic spectra

The purpose of this calculation is to investigate the performance of the MCMC algorithm, so rather than use measured data, dose and charge distributions were calculated using EGS4 (with the same transport parameters as in step 2 of the algorithm) for a monoenergetic 10 MeV broad-beam of electrons (figure 1). A total of 10^7 histories were generated leading to a root-mean-square (rms) statistical error of 0.07% for the dose distribution and 0.45% for the charge distribution as a percentage of dose/ charge maximum.

The MCMC algorithm is run with a range of values of h and n_b. The FWHM acquired are presented in table 1. The rms error is determined from

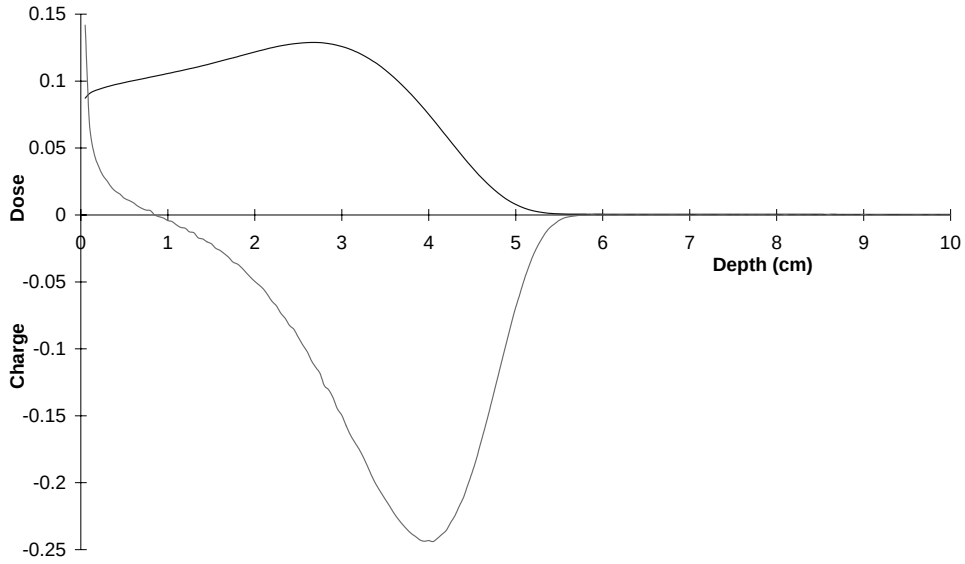

Figure 1: Dose and charge (upper and lower curves respectively) versus depth for a 10.511 MeV broad-parallel beam of electrons calculated with EGS4 using 10^7 histories.

Measurement	Burn-in (n_b)	rms at n_b	Hist./iter. (h)	FWHM
Dose	10^5	0.27%	1	6.9 MeV
	10^5	0.27%	2	4.3 MeV
	10^5	0.27%	3	3.6 MeV
	10^5	0.27%	10	2.3 MeV
	3600	1.8%	100	1.6 MeV
	3600	1.8%	1000	0.66 MeV
	13000	0.8%	50	1.52 MeV
	27000	0.5%	100	1.31 MeV
	27000	0.5%	1000	0.63 MeV
	$.27 \times 10^6$	0.17%	1000	0.61 MeV
	$.27 \times 10^6$	0.17%	10000	0.28 MeV
Charge	10^6	0.59%	1	5.7 MeV
	10^6	0.59%	2	4.1 MeV
	10^6	0.59%	3	3.4 MeV
	10^6	0.59%	10	2.5 MeV
	2800	10%	100	1.77 MeV
	2800	10%	1000	0.66 MeV
	32000	3.3%	100	1.50 MeV
	32000	3.3%	1000	0.87 MeV
	$.3 \times 10^6$	1.1%	100	1.29 MeV
	$.3 \times 10^6$	1.1%	1000	0.87 MeV
	$.3 \times 10^6$	1.1%	10000	0.59 MeV

Table 1: Theoretical resolution (FWHM) of a 10 MeV broad parallel electron source from dose and charge versus depth distributions using the MCMC algorithm for a range of histories per iteration h. At the completion of the burn-in period, n_b, the stated rms error between the calculation and measurement distributions has been achieved.

the sum of square differences between the calculated and measured distributions as a proportion of the dose/ charge maximum. The FWHM have been plotted against $1/\sqrt{h}$ (figure 2) which is proportional to the variance in the additive, T_ε, distributions computed for each iterative step. The limit of the FWHM as this variance goes to zero will give an inherent resolution for the type and quality of measurement. Despite a greater variance in the calculation of charge distributions, the FWHM are similar to those reported for dose distributions.

The smallest resolutions obtained were 0.28 MeV and 0.59 MeV for dose and charge distributions for an rms error of 0.17% and 1.1%, respectively, as a percentage of the dose/charge maximum. The burn-in period was 10^6

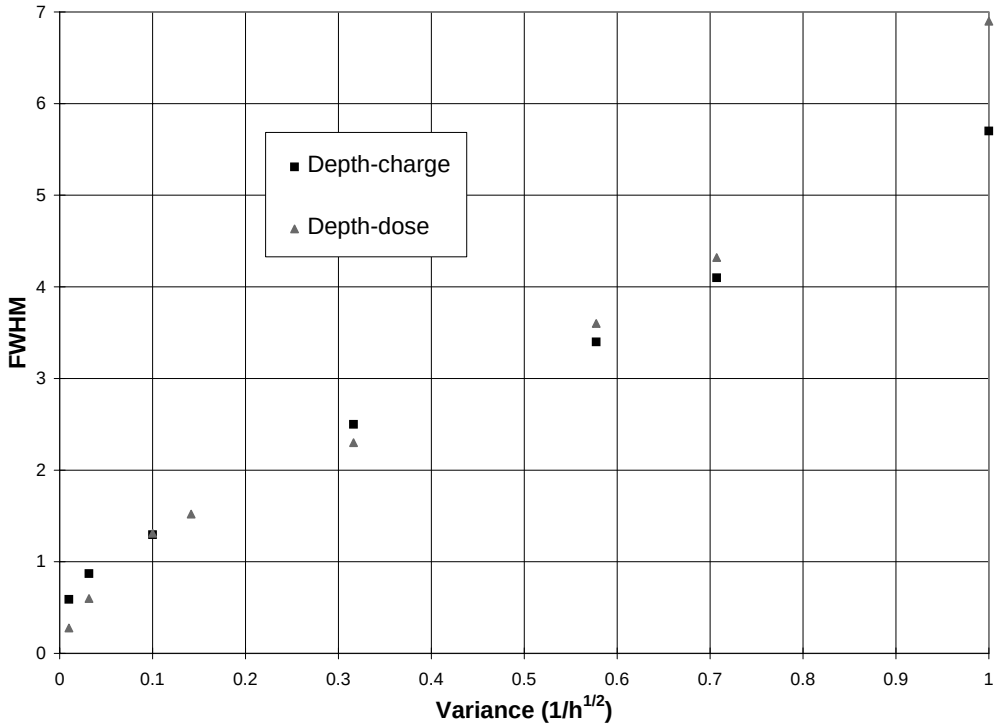

Figure 2: Resolution limits for a 10 MeV monoenergetic electron spectra generated from dose and charge versus depth relationships. The resolution is a function of the variance of the distribution determined for each iterative step which relates to h the number of histories per iteration.

histories after which 10000 histories per iteration were used. These results are potentially compromised by the statistical noise of the "measurement" data set. There is, however, no correlation between the Monte Carlo generated distributions and we would expect the behaviour of the algorithm in these tests to be typical of a measured data set with a normally distributed error.

Bienergetic and realistic spectra

Further studies have been performed with more complex spectra. Firstly, dose versus depth distributions are computed consisting of two monoenergetic sources of equal weighting and examined to demonstrate the resolving power of the method. Secondly, measured depth-dose curves from two therapeutic linear accelerators are examined.

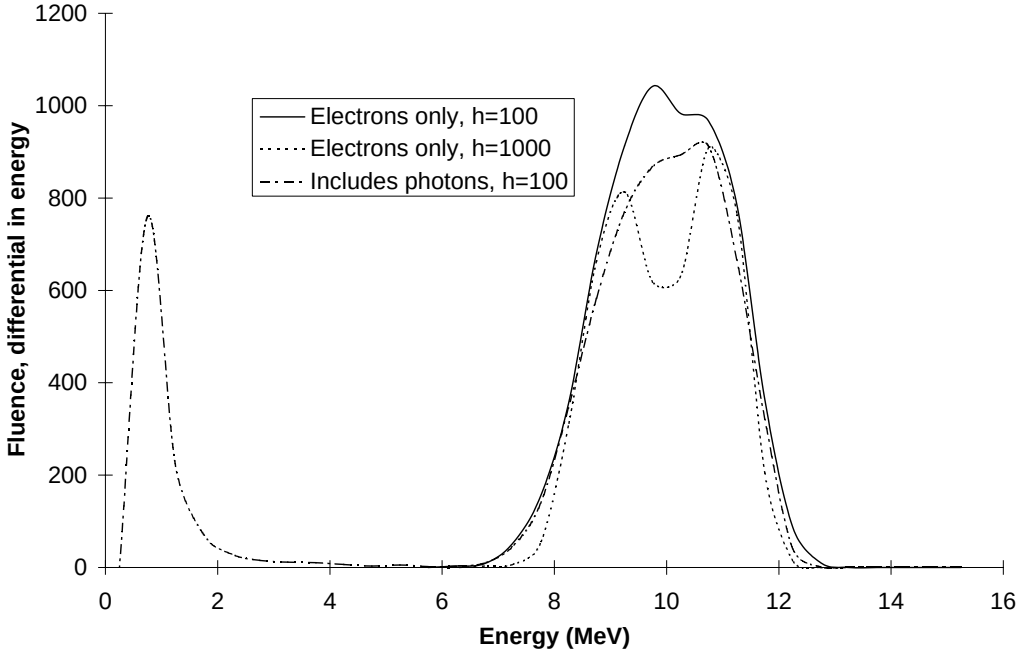

Figure 3: Spectrum determined from a pre-calculated depth-dose distribution comprised of 9 and 11 MeV electrons. The number of histories per iteration is h.

Clear resolution of a 9 and 11 MeV electron source is demonstrated for electrons acquired using batches of 100 and 1000 histories per iteration (figure 3) with theoretical resolutions of 1.31 MeV and 0.61 MeV respectively (from table 1). A third calculation was performed in which the prior distribution, assumed by the MCMC algorithm, was generalised to include a photon component with a uniform distribution. We found that the algorithm is able to exclude such a photon component to 17% of the total fluence and that the resolution of the electron spectrum is slightly degraded.

A 10 and 20 MeV electron source is well resolved (figure 4). The areas under the peaks are equal but the 10 MeV peak is somewhat broader than predicted. The broadening may be due to the larger grid spacing (1 cm) used to accommodate the larger domain. The FWHM resolution is inevitably a function of energy though we have not studied this.

Spectra have been calculated for for a 9 MeV modality of a Varian 2100C

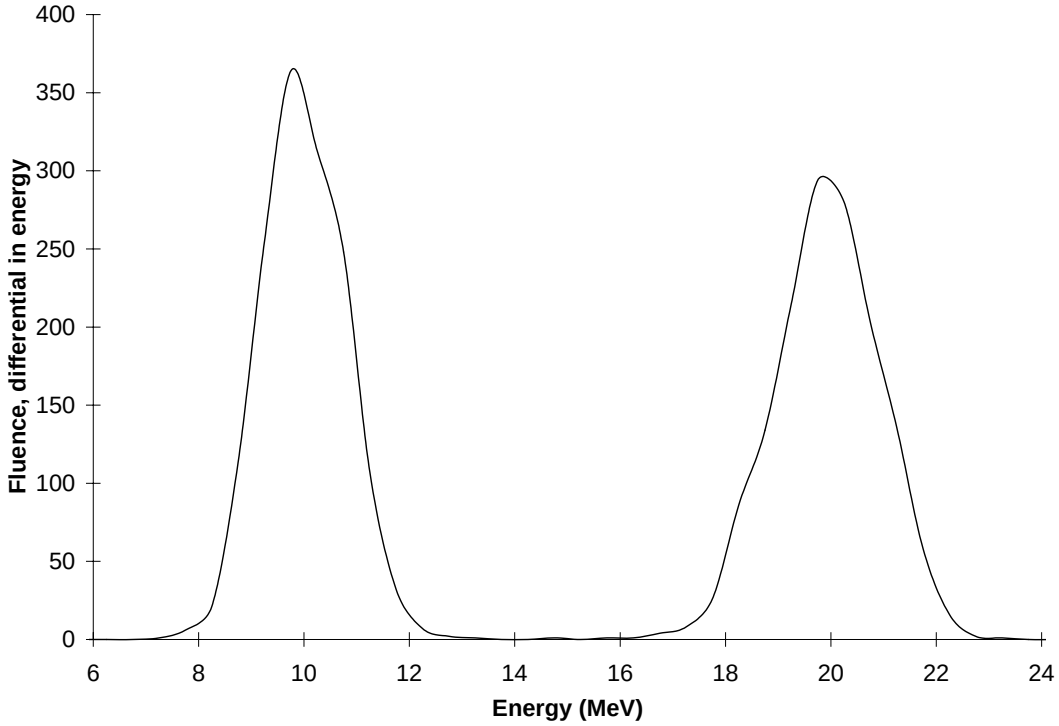

Figure 4: Spectrum determined from a pre-calculated depth-dose distribution comprised of 10 and 20 MeV electrons. A burn-in of 67000 histories followed by batches of 100 histories per iteration have been used. The FWHM for the 10 MeV peak is 1.84 MeV and the 20 MeV peak is 2.36 MeV

(10×10 cm^2 applicator) and a 8 MeV electron modality on a Philips SL15 (14×14 cm^2 applicator) linear accelerators. The depth dose curves have been measured with an NACP chamber(figure 5). Here it is assumed that the beams are broad and parallel. Indeed, electron depth-dose curves at these energies change little with increases in field size beyond 5×5 cm^2. The MCMC algorithm was used with a burn-in of 30000 histories and 100 histories per iteration.

The resulting spectra are shown in figure 6. The photon contamination, i.e. photons which are produced in the head, raises several important issues. The photon component can be treated separately as suggested by various authors [35, 36, 37] but additional photons will be generated in phantom and are difficult to distinguish. It is easier to include photons in the prior distri-

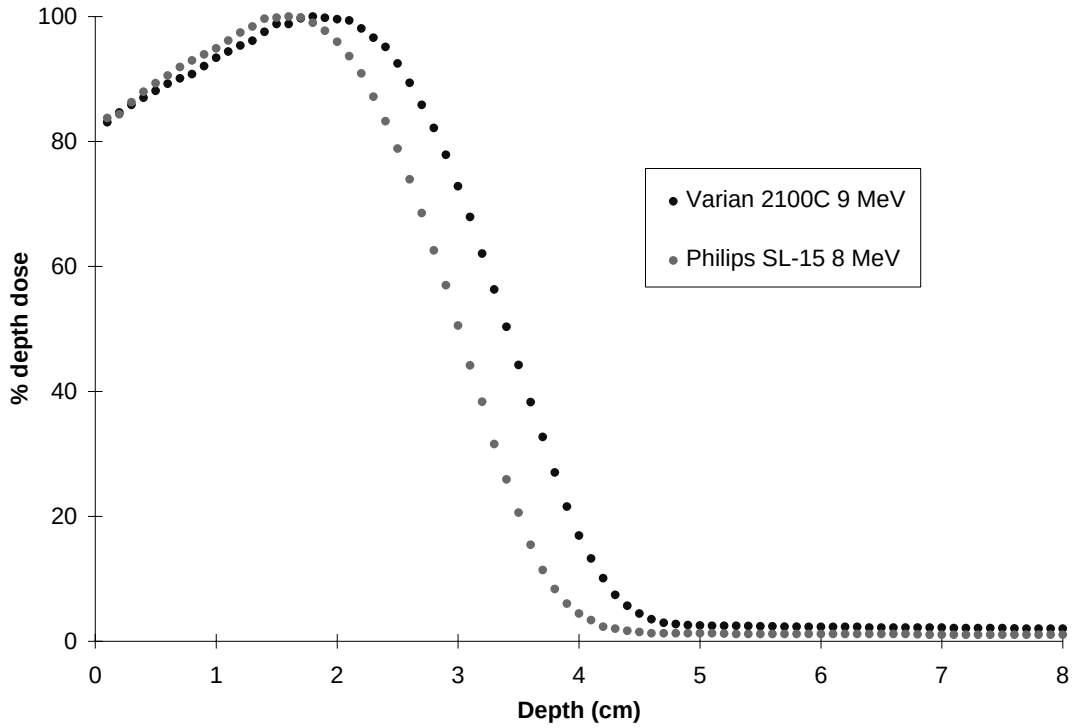

Figure 5: Percentage dose versus depth for the 8 MeV electrons modality on a Philips SL15 with a 14×14 cm^2 applicator and the 9 MeV electrons modality on a Varian 2100C with a 10×10 cm^2 applicator.

bution though the consequence is that some photons will be admitted to the distribution simply because the changes are small enough. The resolution of the photon component will certainly be worse than for an electron spectrum. We have not attempted, in this work, to investigate the ability of the MCMC algorithm to resolve a photon spectrum.

The determination of dose with an ionisation chamber requires a correction for the changes in the relative stopping powers of water and air with depth which may be difficult to determine without the energy spectrum as a function of depth. An alternative is to weight each energy deposition by a restricted mass-collision stopping power ratio and converge instead to a depth-ionisation distribution.

Real charge versus depth measurements have not been analysed here but the techniques described by Roos [38] and Perry et al [39] (see also ICRU-50

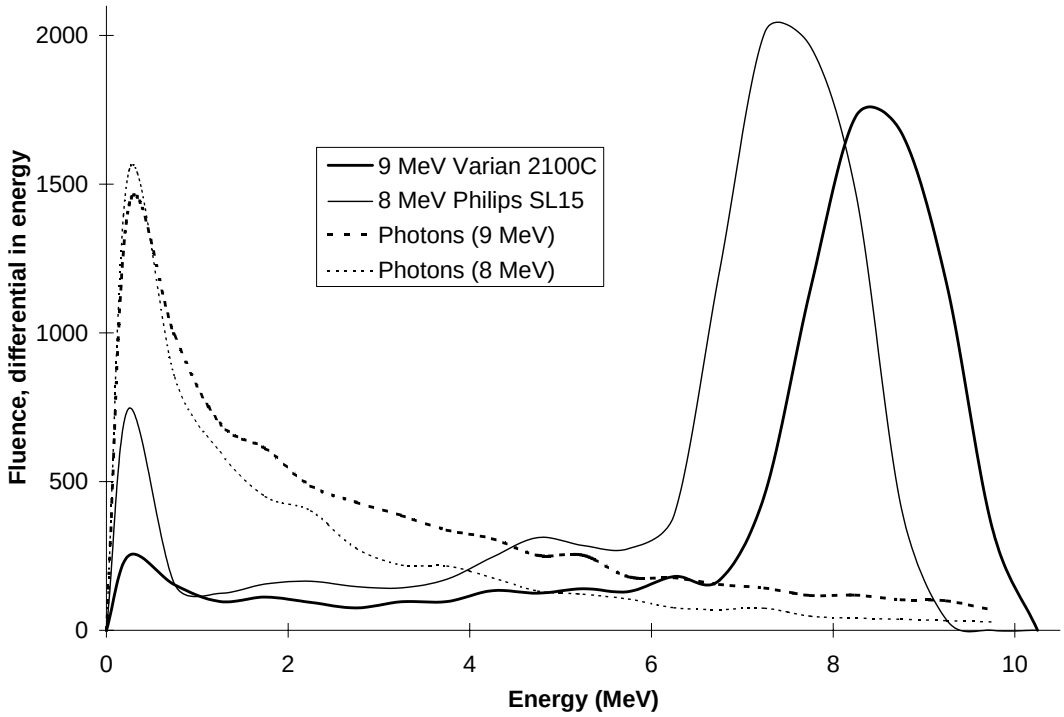

Figure 6: Spectra determined from dose versus depth measurements for the 9 MeV electrons modality on a Varian 2100C and the 8 MeV electrons modality on a Philips SL15. Photons dominate at lower energies but deposite less dose.

[19] for further citations) suggest that accurate measurements can be made of this quantity.

Conclusion

The iterative-inverse/Markov chain Monte Carlo method has been investigated for the in-phantom based determination of electron spectra. The resolution achieved has been shown to be depend on a new parameter - the number of the batched histories per iterative step. We have found no evidence for a fundamental limit to the resolution achievable using the MCMC method. The resolutions achieved in this study at 10 MeV are 0.28 MeV for dose versus depth measures and 0.59 MeV for charge versus depth measures. These results are an upper bound and further investigations are necessary.

References

[1] S. W. Johnsen, P. D. LaRiviere, and E. Tanabe, "Electron depth-dose dependence on energy spectral quality," *Phys. Med. Biol.*, vol. 28, no. 12, pp. 1401–1407, 1983.

[2] J. O. Deasy, P. R. Almond, and M. T. McEllistrem, "The spectral dependence of electron central-axis depth-dose curves," *Med. Phys.*, vol. 21, no. 9, pp. 1369–1376, 1994.

[3] J. O. Deasy, P. R. Almond, M. T. McEllistrem, and C. K. Ross, "A simple magnetic spectrometer for radiotherapy electron beams," *Med. Phys.*, vol. 21, no. 11, pp. 1703–1714, 1994.

[4] J. O. Deasy, P. R. Almond, and M. T. McEllistrem, "Measured electron energy and angular distributions from clinical accelerators," *Med. Phys.*, vol. 23, no. 5, pp. 675–684, 1996.

[5] W. L. Dunn, "Inverse Monte Carlo analysis," *J. Comp. Phys.*, vol. 41, pp. 154–166, 1981.

[6] W. L. Dunn, V. C. Boffi, and F. O'Foghludha, "Applications of the inverse Monte Carlo method in photon beam physics," *Nucl. Instrum. Meth. A*, vol. 255, pp. 147–151, 1987.

[7] A. Piermattei, G. Arcovito, L. Azario, C. Bacci, L. Bianciardi, E. De Sapio, and C. Giacco, "A study of quality of bremsstrahlung spectra reconstructed from transmission measurements," *Med. Phys.*, vol. 17, no. 2, pp. 227–233, 1990.

[8] Y. Zhu and J. Van Dyk, "Accuracy requirements of the primary X-ray spectrum in dose calculations using FFT convolution techniques," *Med. Phys.*, vol. 22, no. 4, pp. 421–426, 1995.

[9] M. Krmar, J. Slivka, I. Bikit, M. Vesković, and L. Conkić, "Evaluation of bremsstrahlung spectra generated by a 4-MeV linear accelerator," *Med. Phys.*, vol. 23, no. 5, pp. 651–654, 1996.

[10] C. R. Baker and K. K. Peck, "Reconstruction of 6 MV photon spectra from measured transmission including maximum energy estimation," *Phys. Med. Biol.*, vol. 42, pp. 2041–2051, 1997.

[11] P. Francois, F. Coste, J. Bonnet, and O. Caselles, "Validation of reconstructed bremsstrahlung spectra between 6 MV and 25 MV from

measured transmission data," *Med. Phys.*, vol. 24, no. 5, pp. 769–773, 1997.

[12] A. Nisbet, H. Weatherburn, J. D. Fenwick, and G. McVey, "Spectral reconstruction of clinical megavoltage photon beams and the implications of spectra determination on the dosimetry of such beams," *Phys. Med. Biol.*, vol. 43, pp. 1507–1521, 1998.

[13] M. D. Altschuler, P. Bloch, E. L. Buhle, and S. Ayyalasomayajula, "3D dose calculations for electron and photon beams," *Phys. Med. Biol.*, vol. 37, no. 2, pp. 391–411, 1992.

[14] A. Kassaee, M. D. Altschuler, S. Ayyalsomayajula, and P. Bloch, "Influence of cone design on the electron beam characteristics on clinical accelerators," *Med. Phys.*, vol. 21, no. 11, pp. 1671–1676, 1994.

[15] R. Martinelli, G. Ghiso, P. Boccacci, F. Foppiano, and L. Andreucci, "Determination of the energy of the electrons incident upon a water phantom to build composite energy beam kernels for 3D dose calculation," in *Proc. Int. Conf. Comp. Radiat. Ther. XI*, (Manchester), pp. 124–125, 1994.

[16] R. P. Hugtenburg, J. R. Turner, and P. H. Butler, "Numerical reconstruction of electron therapy beams," *Med. Phys.*, vol. 22, no. 6, p. 948, 1995.

[17] E. W. Korevaar, J. J. Janssen, P. R. M. Storchi, and H. Huizenga, "Description of a clinical electron beam: The initial phase space as input of the phase space evolution model," *Med. Phys.*, vol. 22, p. 948, 1995.

[18] L. Zhengming and D. Jette, "On the possiblity of determining an effective energy spectrum of clinical electron beams from percentage depth dose (PDD) data of broad beams," *Phys. Med. Biol.*, vol. 44, pp. N177–N182, 1999.

[19] ICRU, *Report 35. Radiation dosimetry: Electron beams with energies between 1 and 50 MeV.* International Commission on Radiation Units and Measurement, 1984.

[20] W. H. Press, *Numerical recipes: The art of scientific computing.* New York: Cambridge University Press, 1986.

[21] L. A. Shepp and Y. Vardi, "Maximum likelihood reconstruction for emission tomography," *IEEE Trans. Med. Imaging*, vol. MI-I, no. 2, pp. 113–122, 1982.

[22] J. Llacer, E. Veklerov, K. J. Coakley, E. J. Hoffman, and J. Nunez, "Statistical analysis of maximum likelihood estimator images of human brain FDG PET studies," *IEEE Trans. Med. Imaging*, vol. 12, no. 2, pp. 215–231, 1993.

[23] Y. Vardi and D. Lee, "From imaging deblurring to optimal investments: Maximum likelihood solutions for positive linear inverse problems," *J. R. Statist. Soc. B*, vol. 55, no. 3, pp. 569–612, 1993.

[24] J. Llacer, "Inverse radiation planning using the dynamically penalized likelihood method," *Med. Phys.*, vol. 24, no. 11, pp. 1751–1764, 1997.

[25] G. H. Olivera, D. M. Shepard, P. J. Reckwerdt, K. Ruchala, J. Zachman, E. E. Fitchard, and T. R. Mackie, "Maximum likelihood as a common computational framework in tomotherapy," *Phys. Med. Biol.*, vol. 43, pp. 3277–3294, 1998.

[26] N. Metropolis, A. W. Rosenbluth, M. N. Rosenbluth, A. H. Teller, and E. Teller, "Equation of state calculations by fast computing machines," *J. Chem. Phys.*, vol. 21, no. 6, pp. 1087–1092, 1953.

[27] W. K. Hastings, "Monte Carlo sampling methods using Markov chains and their applications," *Biometrika*, vol. 57, no. 1, pp. 97–109, 1970.

[28] S. Kirkpatrick, C. D. Gelatt Jr, and M. P. Vecchi, "Optimization by simulated annealing," *Science*, vol. 220, pp. 671–680, 1983.

[29] D. A. Keen and R. L. McGreevy, "Structural modelling of glasses using reverse Monte Carlo simulation," *Nature*, vol. 344, pp. 423–425, 1990.

[30] W. R. Nelson, H. Hirayama, and D. W. O. Rogers, *The EGS4 code system, rep. SLAC-265*. Stanford Linear Accelerator Center, California, 1985.

[31] D. W. O. Rogers, "Low energy electron transport with EGS," *Nucl. Instrum. Meth. A*, vol. 227, pp. 535–548, 1984.

[32] H. Szu and R. Hartley, "Fast simulated annealing," *Phys. Lett. A*, vol. 122, no. 3,4, pp. 157–162, 1987.

[33] M. Oldham and S. Webb, "The optimization and inherent limitations of 3D conformal radiotherapy treatment plans of the prostate," *Brit. J. Radiol.*, vol. 68, pp. 882–893, 1995.

[34] J. Besag, P. Green, D. Higdon, and K. Mengersen, "Bayesian computation and stochastic systems," *Statistical Science*, vol. 10, no. 1, pp. 3–66, 1995.

[35] S. N. Rustgi and J. E. Rodgers, "Analysis of the bremsstrahlung component in 6-18 MeV electron beams," *Med. Phys.*, vol. 14, no. 5, pp. 884–888, 1987.

[36] S. C. Klevenhagen, "An algorithm to include the bremsstrahlung contamination in the determination of the absorbed dose in electron beams," *Phys. Med. Biol.*, vol. 39, pp. 1103–1112, 1994.

[37] B. B. Socini, S. Hyödynmaa, and A. Brahme, "The role of phantom and treatment head generated bremsstrahlung in high-energy electron beam dosimetry," *Phys. Med. Biol.*, vol. 41, pp. 2657–2677, 1996.

[38] B. Roos and M. Karlsson, "Recent developments and future prospects with high energy electrons," in *Clinical electron therapy*, (London), British Institute of Radiology, 1997.

[39] D. Perry, M. Wollin, A. Olch, and A. Buffa, "Range spectra in electron penetration problems," *Med. Phys.*, vol. 25, pp. 43–55, 1998.